Bioorganic & Medicinal Chemistry xxx (xxxx) xxx–xxx

Contents lists available at ScienceDirect

Bioorganic & Medicinal Chemistry

journal homepage: www.elsevier.com/locate/bmc

Pyrrolomycins as antimicrobial agents. Microwave-assisted organic synthesis and insights into their antimicrobial mechanism of action

Maria Valeria Raimondi[a,1], Roberta Listro[b,1], Maria Grazia Cusimano[a,*], Mery La Franca[a,*], Teresa Faddetta[a], Giuseppe Gallo[a], Domenico Schillaci[a], Simona Collina[b], Ainars Leonchiks[c], Giampaolo Barone[a]

[a] Department of Biological, Chemical and Pharmaceutical Sciences and Technologies, (STEBICEF), University of Palermo, via Archirafi 32, 90123 Palermo, Italy
[b] Drug Sciences Department, Medicinal Chemistry and Pharmaceutical Technology Section, University of Pavia, via Taramelli 12, 27100 Pavia, Italy
[c] APP Latvian Biomedical Research and Study Centre (BMC), Rātsupītes iela 1, LV-1067 Rīga, Latvia

ARTICLE INFO

Keywords:
Antimicrobial resistance
Pyrrolomycins
Sortase A
Staphylococcus aureus
In-silico docking studies
MAOS
Pharmacokinetics studies
Murein hydrolase activity

ABSTRACT

New compounds able to counteract staphylococcal biofilm formation are needed. In this study we investigate the mechanism of action of pyrrolomycins, whose potential as antimicrobial agents has been demonstrated. We performed a new efficient and easy method to use microwave organic synthesis suitable for obtaining pyrrolomycins in good yields and in suitable amount for their *in vitro* in-depth investigation. We evaluate the inhibitory activity towards Sortase A (SrtA), a transpeptidase responsible for covalent anchoring in Gram-positive peptidoglycan of many surface proteins involved in adhesion and in biofilm formation. All compounds show a good inhibitory activity toward SrtA, having IC_{50} values ranging from 130 to 300 μM comparable to berberine hydrochloride. Of note compound **1d** shows a good affinity in docking experiment to SrtA and exhibits the highest capability to interfere with biofilm formation of *S. aureus* showing an IC_{50} of 3.4 nM. This compound is also effective in altering *S. aureus* murein hydrolase activity that is known to be responsible for degradation, turnover, and maturation of bacterial peptidoglycan and involved in the initial stages of *S. aureus* biofilm formation.

1. Introduction

Antimicrobial resistance (AMR) is one of the causes for hundreds of thousands of deaths worldwide every year. The new report of the World Health Organization (WHO) in January 2018 deals with the dramatic phenomenon of the antibiotic resistance, and a group of pathogens including Carbapenem-resistant *Enterobacteriaceae* (CRE), *Acinetobacter baumannii*, *Pseudomonas aeruginosa*, *Salmonella*, *Escherichia coli*, *Klebsiella pneumoniae*, *Staphylococcus aureus* etc. are listed on the basis of a priority (critical, high, medium) regarding AMR.[1] Already in October 2015, the WHO launched the new Global Anti-microbiotic Surveillance System (GLASS) in order to deal with growing emergency of super bacteria that do not respond to standard antibiotics. Using the data provided by GLASS, the WHO detected more than 500,000 infection cases in 22 countries.[2]

Adhesion to the host tissues is a step of central importance in bacterial pathogenesis,[3] and novel antimicrobial compounds targeting such mechanism could also be useful to inhibit the formation of biofilms intrinsically resistant to conventional antibiotics. Sortase A (SrtA) is an enzyme of 206 amino acids present in Gram-positive bacteria, which includes an amino-terminal zone (with nonpolar residues) and a catalytic domain for the transpeptidation reaction. Its action consists in

Abbreviations: MAOS, microwave-assisted organic synthesis; SrtA, Sortase A; AMR, antimicrobial resistance; WHO, World Health Organization; GLASS, Global Anti-microbiotic Surveillance System; MSCRAMMs, Microbial Surface Components Recognizing Adhesive Matrix Molecules; FnbpA, fibronectin binding protein A; FnbpB, fibronectin binding protein B; ClfA and ClfB, clumping factors; Can, collagen-binding protein; NBS, *N*-bromosuccinimide; NCS, *N*-chlorosuccinimide; MW, microwave; ADME, absorption distribution metabolism and excretion; DMSO, dimethyl sulfoxide

* Corresponding authors.
E-mail addresses: mariavaleria.raimondi@unipa.it (M.V. Raimondi), roberta.listro01@universitadipavia.it (R. Listro), mariagrazia.cusimano@unipa.it (M.G. Cusimano), mery.lafranca@unipa.it (M. La Franca), teresa.faddetta@unipa.it (T. Faddetta), giuseppe.gallo@unipa.it (G. Gallo), domenico.schillaci@unipa.it (D. Schillaci), simona.collina@unipv.it (S. Collina), ainleo@biomed.lu.lv (A. Leonchiks), giampaolo.barone@unipa.it (G. Barone).
[1] These authors contributed equally to this work.

https://doi.org/10.1016/j.bmc.2019.01.010
Received 7 November 2018; Received in revised form 10 January 2019; Accepted 13 January 2019
0968-0896/ © 2019 Published by Elsevier Ltd.

covalently linking a number of proteins – the Microbial Surface Components Recognizing Adhesive Matrix Molecules (MSCRAMMs) – to peptidoglycan; these are cell wall-associated proteins that have a direct role in the first stage of pathogenesis and biofilm formation. MSCRAMMs are also relevant virulence factors of *S. aureus* because they are involved in pathogenic processes such as evasion of immune defense – due to protein A (SpA) – adhesion to host tissues, such as two fibronectin binding proteins (FnbpA and FnbpB), two clumping factors (ClfA and ClfB) and a collagen-binding protein (Cna). For some of these proteins a key role in biofilm formation has been reported.[5–9] Therefore, SrtA is considered as a good target for the design of new antibacterial drugs, or in general against the bacterial adhesion and the biofilm formation.[4] In 2000, Muzmanian et al. studied knockout mutations of SrtA in *S. aureus*, and they focused their attention on the different modifications of the expression of the protein with LPxTG domain.[5–9] The loss of activity of SrtA with consequent attenuation of virulence are evident in *S. aureus* and also in other important Gram-positive pathogens as *Listeria monocytogenes*, *Streptococcus pneumoniae*, *Streptococcus mutans*.[10–13]

For several years, pyrrolomycins have attracted the attention of the scientific community for their antibacterial properties and for their capability to inhibit the formation of biofilms responsible for the resistance to conventional antibiotics.[14–20] Pyrrolomycins are polihalogenated compounds (Fig. 1) isolated from the fermentation broth of *Actinosporangium* and *Streptomyces* species. They are active against Gram-positive and a few Gram-negative bacterial strains as *Pseudomonas aeruginosa*.[12–14,21–27]

Natural pyrrolomycins, produced by terrestrial and marine microorganisms, are generally active against all preformed staphylococcal biofilms, with percent of inhibition above 60% at the concentration of 1.5 μg/mL[27] Nevertheless, their mechanism of action is still unknown.

We have been active in this field for several years. To discover new active antibacterial agents, we prepared several synthetic pyrrolomycins (Fig. 2), characterized by the presence of chlorine or bromine atoms on the pyrrolomycin scaffold. We observed that their antibacterial property is closely linked to their substitution pattern and that their biological activity is strictly correlated to the different halogenation degree.[12,13,21–23,26–28] Particularly, some of our synthetic pyrrolomycin derivatives showed huge antibacterial activity against *S. aureus*, with MIC in the range of 0.003–0.016 μM.[12,13,21–23,26]

Starting from our previous findings, herein we focus on two natural pyrrolomycins (**C** and **F2a**) and on our most promising synthetic pyrrolomycins (compounds **1d,e,h,i**, see Scheme 1). In detail, we have optimized and scaled-up the synthetic procedure to dispose of an amount of **1d,e,h,i** suitable for in-depth biological investigation. The development of a quick and easy to use methodology for synthesizing pyrrolomycins has a great relevance from a medicinal chemistry standpoint, since the extraction yield from culture broth is slow, moreover, their production is expensive. Indeed, after several controlled pH extractions and chromatographic purifications steps, only 2.5 mg/L of pyrrolomycins from culture broth can be obtained.[14,18–20]

As subsequent step of the research, in order to investigate whether pyrrolmycins **C**, **F2** and **1d,e,h,i** would bind to the active site of SrtA, we performed in silico docking studies using the crystal structure of SrtA and hypothesized the interactions of compounds with the enzyme at the molecular level. Afterwards, we evaluated *in vitro* their ability to interact with SrtA, to inhibit biofilm formation of reference staphylococcal strains and *P. aeruginosa*. For the most interesting compound, the effect on murein hydrolase activity of *S. aureus* extracellular proteins was also evaluated. As a last step of our work we studied the 'drug-likeness' of pyrrolomycins **C**, **F2** and **1d,e,h,i**.

This paper describes the results of our studies.

2. Results

2.1. Chemistry

Pyrrolomycins **1d,e,h,i**, were already obtained by authors using *N*-bromosuccinimide (NBS) or *N*-chlorosuccinimide (NCS) as source of halogen atoms. All reactions were conducted under magnetic stirring for 24 h and at room temperature.[22,23] However, this approach is labor intensive and therefore, a different strategy has been explored to identify a convenient procedure in terms of cost and timing. The main criticism is related to the formation of the intermediates **4,5,6**. Indeed, the reaction is not selective, it gives rise to complex reaction mixtures and, as a consequence, subsequent chromatographic steps are needed to isolate the compounds of our interest.

We then revised the reaction conditions, experimenting the Microwave-Assisted Organic Synthesis (MAOS). So, we have directly verified that MAOS has numerous benefits, including faster chemistry (it reduces reaction times from days or hours to minutes), greater versatility and formation of cleaner products, compared to conventional synthetic methods.[29] Moreover, starting from the observation that the presence of acyl group influences the reactivity of the free positions of the pyrrole, we postulated that the halogenation degree can be appropriately modulated. Accordingly, we performed the reaction by microwave heating, using only one reagent equivalent at a time, isolating the product of interest and then moving on to the subsequent halogenation. This new protocol allowed to increase the yield of O-methylated pyrrolomycins **4b,c**, **5c,d** and **6b,c** up to 93%, and to synthesize the new compounds **4a,d**, **5b,e** and **6d,e** (Table 1). In details, compounds **4a-d** and **5a-e** were obtained by irradiation with a microwave power of 60 W at 90 °C for 5 min. To introduce the halogen in 3-position on the pyrrolic nucleus (compounds **6a-e**) it was necessary to carry out the reaction with four cycles of 15 min each of microwave power of 60 W at 90 °C. The final reaction step, i.e. the O-demethylation, was conducted as previously described, with slight modification, using a large excess of $AlCl_3$ at room temperature, allowing to obtain **1d,e,h,i**, **C** and **F2a** with very good yields (Scheme 1).[22,23]

Analytical and spectroscopic measurements were used to determine the molecular structures of all compounds and the identity of all compounds was confirmed by comparison with spectroscopic literature data.[12,14,19,22-24]

Going into details on new pyrrolomycins **4a,d**, **5b,e** and **6d,e**, in ^{1}H NMR spectra, all compounds showed a singlet attributable to a methoxylic group in the range of 3.72–3.77 δ, signals in the range of 6.51–7.87 δ for the aromatic protons and a broad singlet for the pyrrolic NH in the range of 12.41–13.56 δ, it was verified also by IR spectra that showed a broad band in the range of 3188–3250 cm^{-1}. ^{13}C NMR and elemental analysis confirmed their structures.

It is interesting to note that when compounds **3a-c** react with one molar equivalent of NCS or NBS, the aromatic signal of 3-proton in pyrrolic nucleus shows an unusual chemical shift. In fact, compounds **4a-d** exhibit two doublets in the range of 6.51–6.69 δ for 3-H and 7.33–7.43 δ for 5-H. The 3-proton is more shielded than that awaited from 2-carbonyl pyrroles, probably due to the anisotropic effect of phenyl ring, twisted with respect to the pyrrolic ring. According to what previously observed by Hodge and Rickards,[25] the introduction of chlorine (or bromine) substituents into pyrrole rings causes only minor shifts in the resonance frequencies of the remaining hydrogens.

2.2. Molecular modelling

In order to predict whether pyrrolomycins are able to interact with the active site of SrtA, we performed docking studies using the crystal

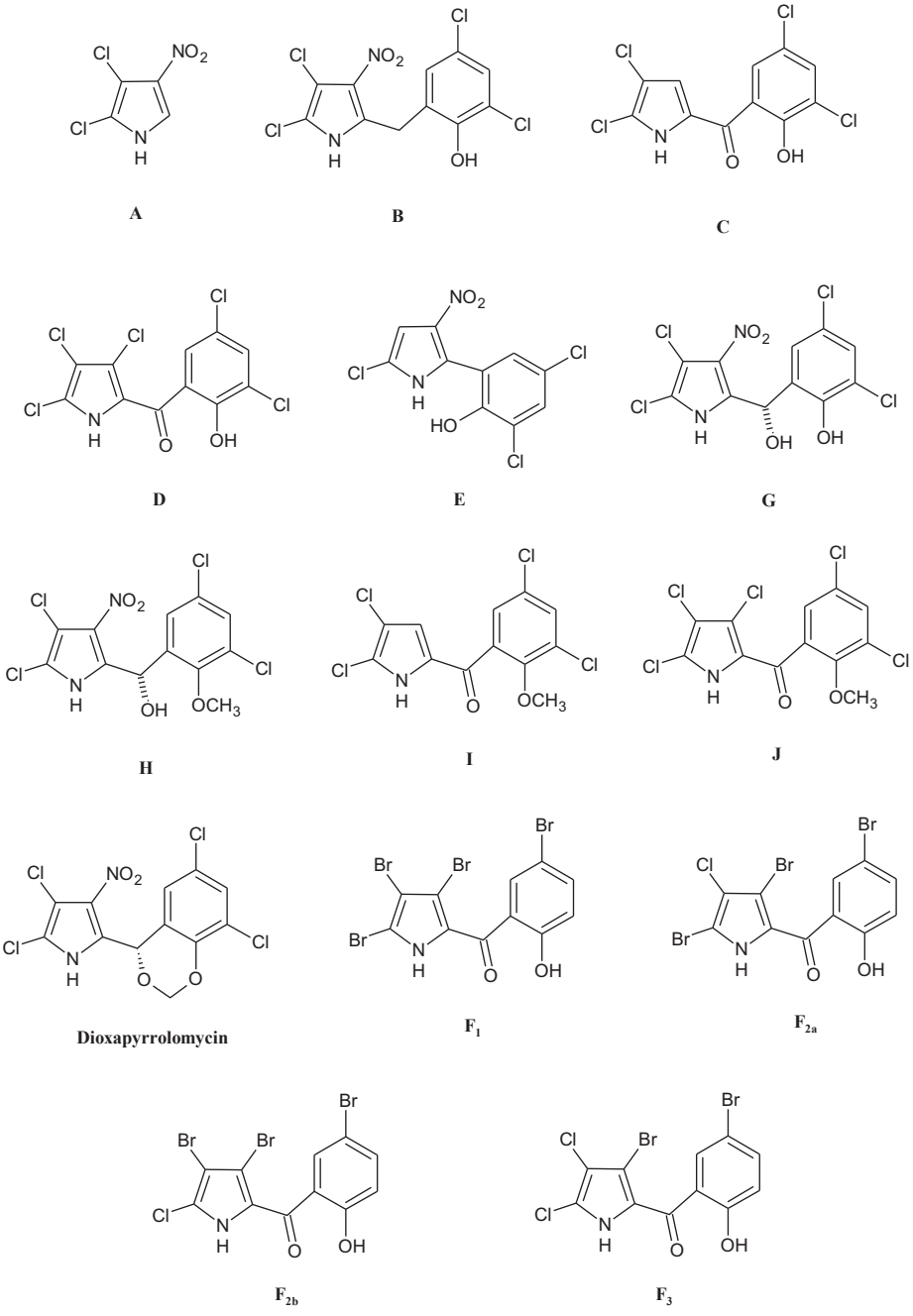

Fig. 1. Structure of natural pyrrolomycins.

structure of PDB-ID: 1T2W.[30] The results obtained suggested that all considered compounds have a similar affinity toward the chain A of SrtA. The picture of the binding complex involving compound **1d** is shown in Fig. 3. In the same figure, the amino acidic residues interacting with the docked molecule are also shown in the insert. In all cases, a hydrogen bond between SER116 and the carbonyl oxygen of pyrrolomycin is also present. Data relative to the other pyrrolomycin compounds are reported in the SI. The studied pyrrolomycins have score values between −6.0 and −6.4 kcal/mol (see Table 3). Given all the above, the designed compounds were considered suitable for the purpose of this study. The analysis of Fig. 3 and of Figs. S1–S6 in the Supplementary Information show that all considered pyrrolomycins are able to similarly bind SrtA, essentially by the combination of both hydrophobic and H-bond interactions.

2.3. Biological investigation

After synthesis and chemical characterization, compounds **1d,e,h,i** together with pyrrolomycins **C** and **F2a** were subjected to biological assays, evaluating their ability to inhibit the enzyme SrtA and the biofilm formation of *S. aureus* ATCC 25923 and of *P. aeruginosa* ATCC 15442.[31]

For testing the SrtA inhibitory activity, the assay checking enzymatic hydrolysis of Srt A FRET substrate analogue dabcyl-QALPETGEE-edans (Table 2) was employed. All compounds resulted active, with IC_{50} values in the range of 130–300 μM. Synthetic pyrrolomycins resulted more effective than natural ones with an IC_{50} comparable to that of the standard berberine hydrochloride (IC_{50} = 120 μM).

Encouraged from these results, we evaluated the capability of pyrrolomycins to inhibit staphylococcal biofilm formation, since the

ARTICLE IN PRESS

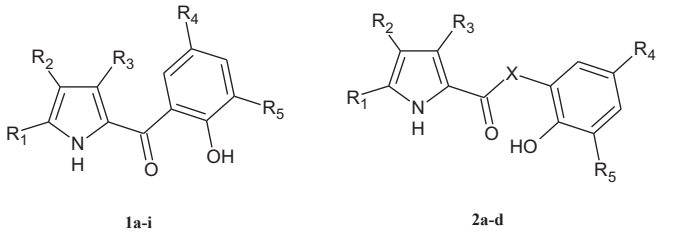

Compound	R_1	R_2	R_3	R_4	R_5	X
1a	Br	Br	H	H	H	-
1b	Br	Br	H	H	Br	-
1c	Br	Br	Br	H	Br	-
1d	Br	Br	Br	Br	Br	-
1e	Br	Br	Br	Cl	Cl	-
1f	Br	Cl	Br	Cl	Cl	-
1g	Cl	Br	Br	Cl	Cl	-
1h	Cl	Cl	Br	Cl	Cl	-
1i	Cl	Br	Cl	Cl	Cl	-
2a	Br	Br	H	Br	Br	CH_2
2b	Br	Br	Br	Br	Br	CH_2
2c	Br	Br	H	Br	Br	CO
2d	Br	Br	Br	Br	Br	CO

Fig. 2. Synthetic pyrrolomycins previously prepared by us.

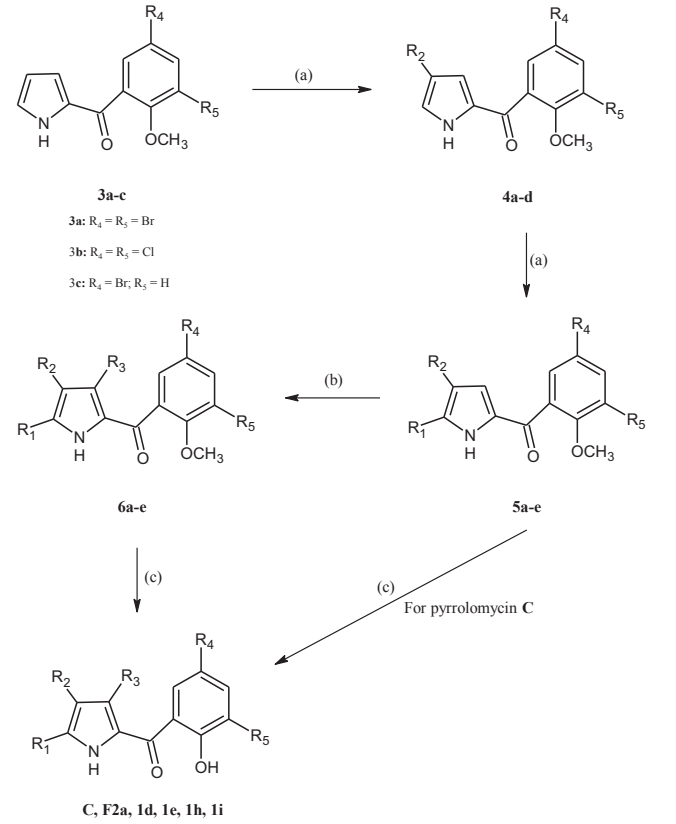

Scheme 1. Experimental protocol to obtain compounds: **4a-d**, **5a-e**, **6a-e**, **C**, **F2a**, **1d**,**e**,**h**,**i**. *Reagents and reaction conditions:* (a) acetonitrile as solvent, equimolar amounts of NBS or NCS, MW heating: 90 °C, 60 W, 5 min; (b) acetonitrile as solvent, equimolar amounts of NBS or NCS, MW heating: 90 °C, 60 W, 4 cycles of 15 min each; (c) dichloromethane anhydrous as solvent, $AlCl_3$ (30 mmol excess), r.t., magnetic stirrer, 12 h; quenching with a 5% H_2SO_4 solution.

interference with growth as a biofilm is strictly related to antivirulence properties of antimicrobial agents. All pyrrolomycins inhibited biofilm formation with inhibition percentages higher than 50% (IC_{50} values are determined and reported in Table 2).

Table 1
Yield for compounds **4a-d**, **5a-e**, **6a-e**, **C**, **F2a**, **1d**,**e**,**h**,**i**.

Compound	R_1	R_2	R_3	R_4	R_5	Previous protocol Yield %[Ref.]	MW Yield %
4a	H	Br	H	Br	Br	–	80
4b	H	Br	H	Cl	Cl	71[22]	83
4c	H	Cl	H	Cl	Cl	61[22]	79
4d	H	Cl	H	Br	H	–	75
5a	Br	Br	H	Br	Br	97[23]	89
5b	Br	Br	H	Cl	Cl	–	83
5c	Cl	Cl	H	Cl	Cl	68[22]	83
5d	Cl	Br	H	Cl	Cl	81[22]	85
5e	Br	Cl	H	Br	H	–	76
6a	Br	Br	Br	Br	Br	98[23]	93
6b	Br	Br	Br	Cl	Cl	68[22]	90
6c	Cl	Cl	Br	Cl	Cl	74[22]	90
6d	Cl	Br	Cl	Cl	Cl	–	91
6e	Br	Cl	Br	Br	H	–	82
C	Cl	Cl	H	Cl	Cl	95[23]	–
F2a	Br	Cl	Br	Br	H	94[23]	–
1d	Br	Br	Br	Br	Br	91[12]	–
1e	Br	Br	Br	Cl	Cl	89[22]	–
1 h	Cl	Cl	Br	Cl	Cl	92[22]	–
1i	Cl	Br	Cl	Cl	Cl	89[12]	–

All tested pyrrolomycins were active in preventing *S. aureus* ATCC 25923 from producing biofilm at IC_{50} values ranging from 3.4 nM to 20.3 μM, in particular the compound **1d** showed the best IC_{50} value (3.4 nM) against *S. aureus*. The pyrrolomycins proved to be selective towards staphylococcal biofilm formation, as *P. aeruginosa* biofilm formation was weakly affected at IC_{50} concentrations ranging from 18.6 to 235.7 μM. The highest potency against *P. aeruginosa* was observed for the compound **1i** whose IC_{50} value was 18.6 μM.

Among all pyrrolomycins, the most active in inhibiting the staphylococcal biofilm were the synthetic pyrrolomycin **1d** (IC_{50} = 3.4 nM) and the natural pyrrolomycin **F2a** (IC_{50} = 8.7 nM), this underlines the importance of the bromine atoms on phenolic ring.

Finally, the most performant pyrrolomycins, in terms of inhibition of biofilm formation (**F2a** and **1d**), were assayed on murein hydrolase activity of *S. aureus* extracellular proteins. Murein hydrolases - hydrolytic enzymes acting in degradation, turnover and maturation of bacterial peptidoglycan - are involved in the initial stages of *S. aureus* biofilm formation.[32,33] In *S. aureus*, the most prominent murein hydrolase is AtlA. that is synthetized as a 137.5 kDa pro-protein cleaved to generate different proteolytic species.[32–34] Indeed, murein hydrolase activity was abolished in *S. aureus AltA* mutants.[32–34] Thus, compound **1d** and **F2a** were added to the inoculated growth medium of *S. aureus* static cultivations at the concentration of 1 μM (≃0.5 μg/mL), respectively. The addition of the compounds caused up to 80% of inhibition of biofilm formation in the respect of untreated cultures after 24 h of incubation. Using the extracellular proteins of the spent medium collected after 24 h of incubation from the treated and untreated *S. aureus* static cultivations, the zymography analysis was carried out and it highlights the activity of a high Mw murein hydrolases (i.e. between 148 and 98 kDa) as a sharp band (Fig. 4a). Furthermore, other appreciable hydrolytic activities can be observed at lower Mw with a total of 6 hydrolysis bands (Fig. 4a). According to the observed inhibition of biofilm formation, the activity of the high Mw murein hydrolase (band 1) diminished at least 2-fold in treated cultivations in the respect of untreated cultivation (Fig. 4b). However, the overall effect of compound **1d** and **F2a** on murein hydrolase activities of *S. aureus* extracellular proteins was not identical but it revealed a different hydrolytic pattern. As an example, an increment of murein hydrolytic activity in correspondence of lower Mw proteins (bands 4, 5 and 6) was observed for the spent medium of **F2a**-treated cultivations (Fig. 4b). According to Sahukhal *et* al. (2015), this last observation could be ascribed to an increased proteolytic activity producing different low Mw Alt species.[32] Interestingly, the increment of murein hydrolytic activity due to low

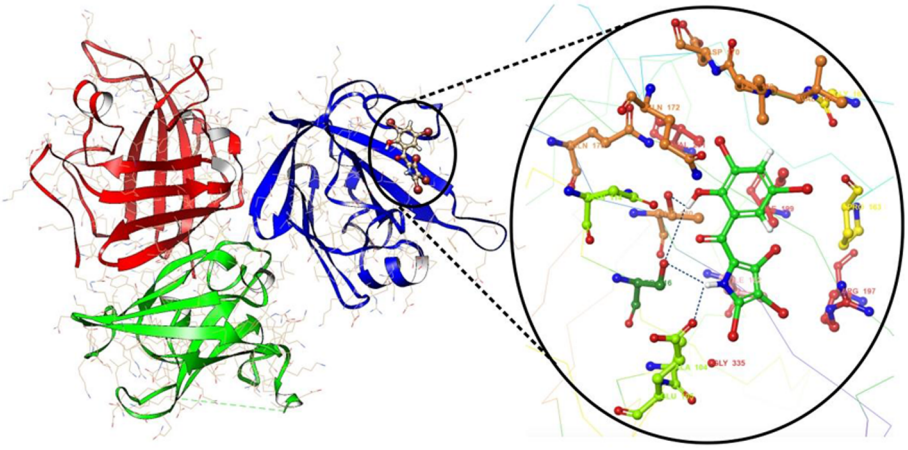

Fig. 3. Best pose of pyrrolomycin **1d**, one of the derivatives with the highest docking score for segment A of Sortase A. In the insert, the amino acidic residues interacting with the molecule are shown.

Table 2
In vitro activity of pyrrolomycins as SrtA inhibitors and IC_{50} values (μM) of tested pyrrolomycins.

	SrtA inhibition	Biofilm inhibition	
Compound	IC_{50} (μM)	*S.aureus* ATCC 25923, IC_{50} (μM)	*P.aeruginosa* ATCC 15442, IC_{50} (μM)
C	300	0.92	235.7
F2a	250	0.0087	78.9
1d	140	0.0034	74.8
1e	130	20.30	106.5
1 h	130	0.10	170.3
1i	160	0.0247	18.6

Table 3
Calculated properties of the selected pyrrolomycins.

	Docking score[a]	%OA[b]	logP [c]	logS[d]	logK[e]	logBB[f]	log IC_{50}[g]
C	−6.1	100	4.475	−5.068	0.381	0.165	−4.524
F2a	−6.0	100	4.256	−5.419	0.420	0.119	−4.419
1d	−6.4	100	4.891	−6.292	0.579	0.347	−4.413
1e	−6.4	100	4.737	−6.083	0.531	0.321	−4.364
1 h	−6.4	100	4.626	−5.679	0.488	0.306	−4.304
1i	−6.4	100	4.594	−5.650	0.481	0.285	−4.294

[a] Best pose score for docking into SrtA (in kcal/mol).
[b] Percentage of oral dose absorbed.
[c] Partition logaritm for octanol/water.
[d] Logarithm for aqueous solubility.
[e] Serum protein binding.
[f] blood–brain barrier permeation as pLog.
[g] HERG K+ channel blockage.

Mw protein species is associated with increased cell death and a defect in biofilm maturation.[32] Therefore, this analysis showed a common negative effect on the activity of the high Mw hydrolase (band 1) of both compounds and, more in general, a compound-specific effect on the overall murein hydrolase activities that paralleled the inhibition of biofilm formation.

2.4. In silico ADME properties

Often, promising potential drugs fail because of unsatisfactory ADME properties, so we performed studies in silico to predict ADME and toxicity, starting from the docking complexes (see paragraph 2.2). Molecular descriptors were computed to predict six physicochemical properties of each pyrrolomycin compound (Table 3): (b) percentage of oral dose absorbed (%OA); (c) partition coefficient (ClogP); (d) logarithm for aqueous solubility (ClogS); (e) serum protein binding (ClogK); (f) blood–brain barrier permeation as pLog (ClogBB); (g) HERG K + channel blockage. These parameters are the most representative features to determine the ADME profile. In Table S1 of Supplementary Information, the calculated ADME properties of the considered pyrrolomycin molecules have been summarized. Almost all parameters taken into consideration, with the exception of the weakly polar component of SASA and of the possibility to accept H-bonds, are included within the range of properties of 95% of known drugs. The results obtained show that the considered pyrrolomycins are promising drug candidates. The values of Human Oral Absorption reported in Table S1 are 100% for all pyrrolomycins considered. This result indicates that these compounds could be orally administered drugs. In general, all parameters reported in Table S1 show that they all possess optimal pharmacokinetic properties. Since the reference values of serum protein binding constant (logK) are within the range −1.5 – 1.5, the results show that all the title compounds possess an optimal value of binding to plasmatic proteins.

3. Conclusions

In the present paper, we identified two pyrrolomycins as promising antimicrobial agents. Of particular interest is compound **1d**, for which a quick, easy to use and scalable synthetic methodology was developed. Conversely, the extraction procedure of **F2a** from culture broth is slow and expensive.

The results of molecular modelling studies and enzymatic assays have confirmed the involvement of SrtA in the biological activity of pyrrolomycins. In particular, the results of the computational investigations, and the analysis of the binding modes, show that the title compounds can be promising drug candidates to be used to treat infections. Results on the inhibition of staphylococcal biofilm formation, coupled with an altered pattern of murein hydrolase activity, have shown the antivirulence property of pyrrolomycins.

Lastly, results of in silico drug likeness study evidenced that both compounds have good ADME properties, thus prompting us to further studies.

4. Experimental section

4.1. Chemistry

4.1.1. Materials and instruments

Melting points were determined on a Büchi 530 capillary melting

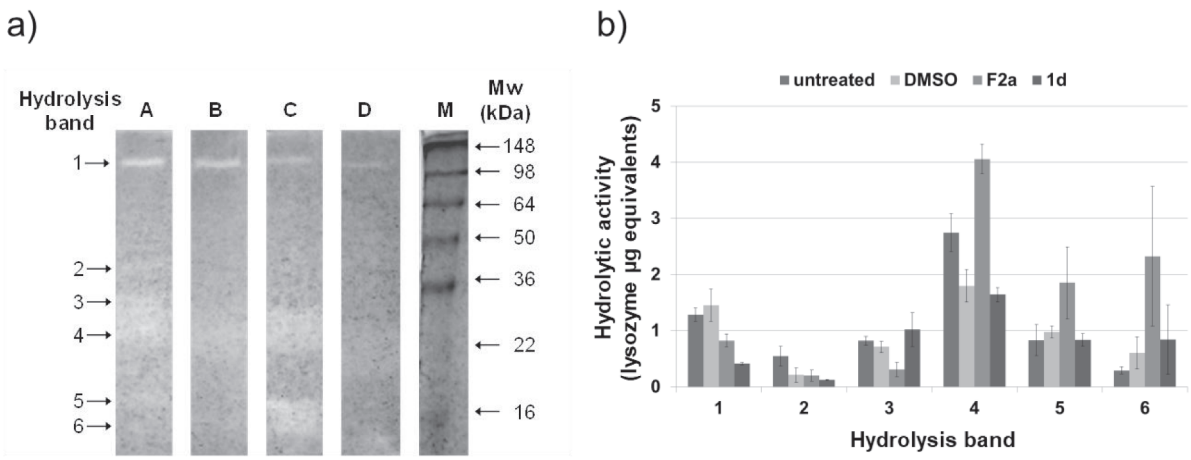

Fig. 4. Zymography assay of *S. aureus* extracellular proteins. Panel a): murein hydrolytic activity was assayed using extracellular proteins of spent medium aliquots that were collected from static cultivations untreated (A) or treated with 0.1% DMSO (B), 1 µM **F2a** (C) and 1 µM compound **1d** (D). Panel b): murein hydrolase activity was quantified as lysozyme µg equivalents based on electrophoretic band intensities.

point apparatus and are uncorrected. IR spectra were recorded at room temperature in Nujol mulls with a Perkin Elmer Infrared 137 E spectrometer. ^{1}H NMR (300 MHz) and APT (75 MHz) spectra were recorded with a Bruker AC-E spectrometer at room temperature in DMSO-d_6, unless otherwise specified, using tetramethylsilane as internal standard; chemical shifts (δ) are expressed as ppm values. Microwave reactions were performed with an Anton Paar GmbH - Monowave 300 (Microwave synthesis reactor). Microanalyses (C, H, N) were carried out with Elemental Vario EL III apparatus and were in agreement with theoretical values ± 0.4%. All reactions were monitored by TLC on precoated aluminium sheets 20 × 20 (0.2 mm Kieselgel 60 G F254, Merck) and C-18 reverse phase (RP-18 F254, Merck) using UV light at 254 nm for visualization. All reagents and solvents were from Aldrich, Fluka, Merck, Across or J.T. Baker.

4.1.2. Methods

Known pyrrolomycins **1d,e,h,i**, **C**, **F2a**, **4b,c**, **5a,c,d** and **6a-c** were prepared and characterized as previously described.[12,14,19,22–24]

*4.1.2.1. General procedure for preparation of substituted (2-methoxyphenyl-1H-pyrrol-2-yl)methanones **(4a,d, 5b,e, 6d,e)** under microwave heating.* To a solution of 1 mmol of **3a-c** in 5 mL of acetonitrile, 1 mmol of crystallized NBS or NCS was added. The reaction mixture was irradiated with a microwave power of 60 W at 90 °C for 5 min (compounds **4a-d** and **5a-e**) or 60 W at 90 °C for 4 cycles of 15 min each (compounds **6a-e**). The reaction mixture was evaporated under reduced pressure and the residue was partitioned between water (10 mL) and diethyl ether (10 mL) and, subsequently, extracted twice with diethyl ether (10 mL). The combined extracts were washed with water, dried over anhydrous sodium sulfate and evaporated. The crude product was crystallized from ethanol.

*4.1.2.1.1. (4-bromo-1H-pyrrol-2-yl)(3,5-dibromo-2-methoxyphenyl) methanone **(4a)**.* White solid, Yield 80%, mp 116 °C. ^{1}H NMR: δ 3.71 (s, 3H, OCH_3), 6.67 (s, 1H, H-3), 7.48 (s, 1H, H-5), 7.49 (d, 1H, H-6', J_m = 2.5 Hz), 7.81 (d, 1H, H-4', J_m = 2.5 Hz), 12.58 (br s, 1H, NH). ^{13}C NMR (acetone-d_6): δ 62.1, 113.5, 118.1, 124.2, 127.4, 128.6, 130.7, 131.4, 135.9, 152.7, 180.4, 205.2. IR (cm^{-1}): 3250 (NH), 1630 (CO). Anal. calc. for $C_{12}H_8Br_3NO_2$: C, 32.91%; H, 1.84%; N, 3.20%. Found: C, 33.05%; H, 1.93%; N, 3.24%.

*4.1.2.1.2. (5-bromo-2-methoxyphenyl)(4-chloro-1H-pyrrol-2-yl) methanone **(4d)**.* White solid, Yield 75%, mp 115–116 °C. ^{1}H NMR: δ 3.73 (s, 3H, OCH_3), 6.51 (s, 1H, H-3), 7.12 (d, 1H, H-3', J_o = 8.95 Hz), 7.33 (s, 1H, H-5), 7.45 (d, 1H, H-6', J_m = 2.35 Hz), 7.65 (dd, 1H, H-4', J_o = 8.92 Hz, J_m = 2.3 Hz), 12.41 (br s, 1H, NH). ^{13}C NMR (acetone-d_6): δ 62.1, 113.8, 118.2, 124.3, 127.4, 128.6, 130.7, 131.5, 136.0, 152.8, 180.5, 205.3. IR (cm^{-1}): 3242 (NH), 1619 (CO). Anal. calc. for $C_{12}H_9BrClNO_2$: C, 45.82%; H, 2.88%; N, 4.45%. Found: C, 45.87%; H, 2.93%; N, 4.44%.

*4.1.2.1.3. (4,5-dibromo-1H-pyrrol-2-yl)(3,5-dichloro-2-methoxyphenyl)methanone **(5b)**.* White solid, Yield 83%, mp 162–163 °C. ^{1}H NMR: δ 3.71 (s, 3H, OCH_3), 6.80 (s, 1H, H-3), 7.51 (d, 1H, H-6', J_m = 2.5 Hz), 7.82 (d, 1H, H-4', J_m = 2.5 Hz), 13.58 (br s, 1H, NH). ^{13}C NMR (acetone-d_6): δ 62.1, 96.4, 121.6, 127.4, 128.6, 129.0, 130.4, 131.5, 135.4, 152.7, 179.7, 206.4. IR (cm^{-1}): 3188 (NH), 1616 (CO). Anal. calc. for $C_{12}H_7Br_2Cl_2NO_2$: C, 33.68%; H, 1.65%; N, 3.27%. Found: C, 33.78%; H, 1.71%; N, 3.36%.

*4.1.2.1.4. (5-bromo-4-chloro-1H-pyrrol-2-yl)(5-bromo-2-methoxyphenyl)methanone **(5e)**.* White solid, Yield 76%, mp 134–135 °C. ^{1}H NMR: δ 3.73 (s, 3H, OCH_3), 6.58 (s, 1H, H-3), 7.10 (d, 1H, H-3', J_o = 8.7 Hz), 7.46 (d, 1H, H-6', J_m = 2.5 Hz), 7.63 (dd, 1H, H-4', J_o = 8.75 Hz, J_m = 2.45 Hz), 13.28 (br s, 1H, NH). ^{13}C NMR (acetone-d_6): δ 62.2, 96.4, 113.78, 121.7, 127.5, 128.7, 129.0, 130.5, 131.6, 135.4, 179.8, 206.4. IR (cm^{-1}): 3206 (NH), 1611 (CO). Anal. calc. for $C_{12}H_8Br_2ClNO_2$: C, 36.63%; H, 2.05%; N, 3.56%. Found: C, 36.78%; H, 2.13%; N, 3.63%.

*4.1.2.1.5. (4-bromo-3,5-dichloro-1H-pyrrol-2-yl)(3,5-dichloro-2-methoxyphenyl)methanone **(6d)**.* White solid, Yield 91%, mp 193–194 °C. ^{1}H NMR: δ 3.78 (s, 3H, OCH_3), 7.58 (d, 1H, H-6', J_m = 2.6 Hz), 7.87 (d, 1H, H-4', J_m = 2.6 Hz), 13.86 (br s, 1H, NH). ^{13}C NMR (acetone-d_6): δ 61.88, 105.1, 113.6, 121.1, 127.2, 128.8, 129.1, 131.6, 135.5, 152.5, 179.6, 205.4. IR (cm^{-1}): 3201 (NH), 1626 (CO). Anal. calc. for $C_{12}H_6BrCl_4NO_2$: C, 34.49%; H, 1.45%; N, 3.35%. Found: C, 34.58%; H, 1.51%; N, 3.43%.

*4.1.2.1.6. (5-bromo-2-methoxyphenyl)(3,5-dibromo-4-chloro-1H-pyrrol-2-yl)methanone **(6e)**.* White solid, Yield 82%, mp 184–185 °C. ^{1}H NMR: δ 3.73 (s, 3H, OCH_3), 7.10 (d, 1H, H-3', J_o = 9.15 Hz), 7.46 (d, 1H, H-6', J_m = 2.5 Hz), 7.67 (dd, 1H, H-4', J_o = 9.2 Hz, J_m = 2.5 Hz), 13.67 (br s, 1H, NH). ^{13}C NMR (acetone-d_6): δ 55.6, 103.8, 106.6, 107.5, 112.1, 113.7, 130.1, 130.9, 134.4, 156.6, 180.7, 205.2. IR (cm^{-1}): 3207 (NH), 1611 (CO). Anal. calc. for $C_{12}H_7Br_3ClNO_2$: C, 30.51%; H, 1.49%; N, 2.97%. Found: C, 30.62%; H, 1.58%; N, 3.08%.

*4.1.2.2. General procedure for preparation of pyrrolomycins **C, F2a, 1d,e,h,i.**[12,22,23].* In a typical experiment, to a solution of 1 mmol of **6a-e** (or **5c** for pyrrolomycin **C**) in 20 mL of anhydrous dichloromethane in an ice-salt bath, 4 g of $AlCl_3$ (30 mmol) was added. The reaction mixture was left to stir overnight at room temperature. The solution was cautiously decomposed with ice-

sulfuric acid 5% (30 mL), then 50 mL of diethyl ether was added. The mixture was stirred vigorously for 10 min, the organic layer was separated and the aqueous phase extracted with diethyl ether (2x30 mL). The combined extracts were washed with water until neutrality, dried over anhydrous sodium sulfate, and evaporated. The crude product was crystallized from dichloromethane to give pure pyrrolomycins. The yields coincide with those reported in the literature.[12,22,23]

4.2. Molecular modelling

The molecular structures have been drawn with the Avogadro program, version 1.2.0,[35] while their geometry optimization was performed with the LigPrep routine of the Maestro Schrödinger Suite version 2017-4.[36]

The X-ray crystallographic structure of SrtA (Fig. 3) was obtained from the Protein Data Bank,[37] PDB-ID: 1T2W.[30] The chosen structure of SrtA is complexed with the LPETG peptide, since it has been reported that all SrtA inhibitors bind the protein similarly to such peptide.

All co-crystallized water molecules and counterions were removed from the PDB protein structure and non-resolved hydrogen atoms were added in some amino acid residues.

The Chimera program,[38] UFCS Chimera version 1.11.2, was used to create the pdb files of the ligands and of SrtA. Molecular docking calculations were performed with Autodock Vina [39] on the protein binding site of the LPETG inhibitor. Pharmacokinetic studies, to estimate the Absorption, Distribution, Metabolism, and Excretion (ADME) and the toxicity of the ligands, were performed with QikProp routine of Maestro.[36]

4.3. Biological evaluation

4.3.1. Screening as Sortase A (SrtA) inhibitors

All of the compounds were prepared as 10 mM stock solutions in dimethyl sulfoxide (DMSO) and used for the IC_{50} determination. The compounds were tested at concentrations ranging from 200 to 20 μM in black 384-well plates (Greiner Bio-One). Berberine chloride, a known Sortase A inhibitor, was used as the positive control.[40] The inhibitory activity of all the compounds was assessed by quantifying the increase in fluorescence intensity upon cleavage of the FRET-peptide dabcyl-QALPETGEE-edans, which was used as the sortase substrate. A previously published method [40,41] was used with slight modifications. Briefly, the reactions were performed in a volume of 100 μL containing 50 mM Tris-HCl, 5 mM $CaCl_2$, 150 mM NaCl, pH 7.5, 10 μM *S. aureus* SrtA, 20 μM fluorescent peptide substrate dabcyl-QALPETGEE-edans, and the prescribed concentrations of the test compounds or positive controls. The peptide substrate without the recombinant SrtA was incubated in the same manner and used as a negative control. The reactions were conducted for 24 h at 37 °C, and the fluorescence emitted with an excitation wavelength of 350 nm and an emission wavelength of 495 nm after substrate cleavage was recorded. End-point determination of product formation was used as a criterion for the primary screening. This determination was made by measuring the total product fluorescence 24 h after the initiation of the reaction. The relative inhibition activity was determined as $\%I = 100\% - (F_{sample}/F_{control}*100\%)$, where F_{sample} is the fluorescence intensity of the well containing the corresponding test compound and $F_{control}$ is the fluorescence of the positive control reaction without inhibition. For the IC_{50} determination, 10 μM *S. aureus* SrtA was preincubated in the reaction buffer with increasing concentrations of the inhibitory compounds (x–y μM) for 1 h at 37 °C prior to the addition of the dabcyl-QALPETGEE-edans substrate to a final concentration of 50 μM. The total fluorescence was recorded at 1-min intervals for 1 h, and the progress curves were constructed. The initial velocities of the biphasic reactions were obtained through nonlinear regression. The IC_{50} values were determined by fitting the obtained data to the following default four-parameter variable slope sigmoidal function in SigmaPlot 12.5 using a nonlinear least squares algorithm.

$$y = \min + \frac{(\max - \min)}{1 + (x/IC50)^{-HillSlope}}$$

4.3.2. Inhibition of biofilm formation (Crystal violet method)

Bacterial strains *S. aureus ATCC 25923* and *P. aeruginosa* ATCC 15442 were incubated in test tubes with Tryptic Soy Broth (TSB) (5 mL) containing 2% w/v glucose at 37 °C for 24 h. After that, the bacterial suspensions were diluted to achieve a turbidity equivalent to a 0.5 McFarland standard. The diluted suspension (2.5 μL) was added to each well of a single cell culture polystyrene sterile, flat-bottom 96-well plate filled with TSB (100 μL) with 2% w/v glucose. A screening concentration of 100 μg/mL of all compounds were directly added to the wells to assess inhibition percentages values, or in the case of determination of IC_{50} (concentration at which a percentage of inhibition equal to 50% is observed), concentrations in the range among 100 and 0.001 μM. Plates were incubated at 37 °C for 24 h. After biofilm growth, the content of each well was removed, wells were washed twice with sterile PBS 1X and stained with 150 μL of 0.1% w/v crystal violet solution for 30 min at room temperature. Excess solution was removed and the plate was washed twice using tap water. A volume of 125 μL of acetic acid of 33% v/v was added for 15 min to each stained well to solubilize the dye. Optical density (OD) was read with wavelength of 540 nm using a microplate reader (Glomax Multidetection System Promega).

All tests involved two replicates and were repeated in at least three independent experiments. The percentage of inhibition was calculated through the formula:

$$\%\ of\ inhibition = [(OD\ growth\ control - OD\ sample)/OD\ growth\ control] \times 100$$

4.3.3. Murein hydrolase assays

S. aureus [10^8 cfu/mL] was inoculated in 5 mL of TSB containing 2% (w/v) glucose and incubated overnight at 37 °C with shaking (200 rpm). To evaluate the effect on *S. aureus* murein hydrolytic activity, an aliquot of 20 μL of culture was inoculated into 2 mL of TSB with 2% (w/v) glucose containing 1 μM of compound **1d** or **F2a** in flat 24-well polystyrene cell culture plate (Costar). Compound **1d** and **F2a** were prepared as 0.5 μg/μL stock solutions in DMSO. Untreated and 0.1% (v/v) DMSO-containing *S. aureus* cultivations were used as control conditions. The test and control cultivations were performed in triplicated replicas. The cell culture plate was incubated statically at 37 °C for 24 h. Following incubation, spent medium samples were collected without taking well-surface adherent cells. The samples were centrifuged (10 min at 2000 *rcf*) to separate possible planktonic cells and, then, 1 mL of supernatants was lyophilized and suspended in 200 μL of 1 M Tris-HCl buffer (pH 7.4). The activity of extracellular murein hydrolases were assayed by zymographic analyses as previously described using lysozyme as positive control.[33] In particular, 10 μL for each sample was separated using SDS-PAGE on a 12% acrylamide gel containing 1 mg/mL *Micrococcus lysodeikticus* ATCC No 4698 cells (Sigma Aldrich, St. Louis, MO) at 100 V for approximately 2 h. After electrophoresis, the gel was washed twice in 100 mL of H_2O for 30 min at room temperature under constant agitation. After washing, the gel was incubated with renaturing buffer (20 mM Tris, 50 mM NaCl, 20 mM $MgCl_2$, 0.5% Triton X-100, pH 7.4) for 30 min at room temperature and then for 24 h at 37 °C with replaced renaturing buffer under constant agitation until clear hydrolytic bands appeared (between 16 h and 48 h). To highlight the presence of digestion bands, the gels were stained with 0.1% Methylene Blue (Sigma-Aldrich). Thus, bands without staining were indicative of muerein hydrolysis. In particular, *S. aureus* hydrolytic activity was calculated using triplicate measurements by ImageJ [42] analysis performed on digitalized zymography images and was reported as lysozyme μg equivalents.

Acknowledgments

This work was supported by Ministero dell'Istruzione dell'Università e della Ricerca (MIUR) of the Italian Government [grant number PJ_RIC_FFABR_2017_160599]. A special thanks to Professor Salvatore Petruso for His valuable advice.

Author contributions

M.V.R., D.S. and G.B. conceived the work and were responsible for the correctness of the whole study. M.V.R., M.G.C. and G.G. were responsible for the experimental design and for data analysis of the whole study. A.L., R.L., M.G.C., T.F. and M.L.F. performed the experiments. M.V.R., D.S., G.B., and S.C. wrote and revised the manuscript.

Conflict of interest

The authors declare no competing financial interest.

Appendix A. Supplementary data

Supplementary data to this article can be found online at https://doi.org/10.1016/j.bmc.2019.01.010.

References

1. Jan 29, C. D. | N. R. | C. N. |; 2018. WHO releases its first report on global antibiotic resistance http://www.cidrap.umn.edu/news-perspective/2018/01/who-releases-its-first-report-global-antibiotic-resistance. (accessed 2.05.18.).
2. Organization, W. H. O. Global Antimicrobial Resistance Surveillance System (GLASS) Report: Early Implementation 2016–2017; World Health Organization, 2018. Number of pages: 164. ISBN: 978-92-4-151344-9. http://www.who.int/glass/resources/publications/early-implementation-report/en/ (accessed 2.05.18.).
3. Dodson KW, Pinkner JS, Rose T, Magnusson G, Hultgren SJ, Waksman G. Structural basis of the interaction of the pyelonephritic E. Coli adhesin to its human kidney receptor. *Cell.* 2001;105(6):733–743. https://doi.org/10.1016/S0092-8674(01)00388-9.
4. Cascioferro S, Raffa D, Maggio B, Raimondi MV, Schillaci D, Daidone G. Sortase A inhibitors: recent advances and future perspectives. *J Med Chem.* 2015;58(23):9108–9123. https://doi.org/10.1021/acs.jmedchem.5b00779.
5. Mazmanian SK, Liu G, Jensen ER, Lenoy E, Schneewind O. Staphylococcus Aureus Sortase mutants defective in the display of surface proteins and in the pathogenesis of animal infections. *Proc Natl Acad Sci USA.* 2000;97(10):5510–5515. https://doi.org/10.1073/pnas.080520697.
6. Oh K-B, Oh M-N, Kim J-G, Shin D-S, Shin J. Inhibition of sortase-mediated *Staphylococcus aureus* adhesion to fibronectin via fibronectin-binding protein by sortase inhibitors. *Appl Microbiol Biotechnol.* 2006;70(1):102–106. https://doi.org/10.1007/s00253-005-0040-8.
7. Sibbald MJJB, Yang X-M, Tsompanidou E, et al. Partially overlapping substrate specificities of staphylococcal group A sortases. *Proteomics.* 2012;12(19–20):3049–3062. https://doi.org/10.1002/pmic.201200144.
8. Bierne H, Mazmanian SK, Trost M, et al. Inactivation of the SrtA gene in listeria monocytogenes inhibits anchoring of surface proteins and affects virulence. *Mol Microbiol.* 2002;43(4):869–881. https://doi.org/10.1046/j.1365-2958.2002.02798.x.
9. A.S. Kharat A. Tomasz Inactivation of the SrtA Gene affects localization of surface proteins and decreases adhesion of Streptococcus pneumoniae to human pharyngeal cells in vitro Infect Immun 2003 71 5 2758 2765 https://doi.org/ 10.1128/IAI.71.5.2758-2765.2003.
10. Hu P, Huang P, Chen WM. Curcumin inhibits the Sortase A activity of the *Streptococcus mutans* UA159. *Appl Biochem Biotechnol.* 2013;171(2):396–402. https://doi.org/10.1007/s12010-013-0378-9.
11. Vanier G, Sekizaki T, Domínguez-Punaro MC, et al. Disruption of SrtA gene in streptococcus suis results in decreased interactions with endothelial cells and extracellular matrix proteins. *Vet Microbiol.* 2008;127(3–4):417–424. https://doi.org/10.1016/j.vetmic.2007.08.032.
12. Petruso S, Bonanno S, Caronna S, Ciofalo M, Maggio B, Schillaci D. Oxidative halogenation of substituted pyrroles with Cu(II). Part IV. bromination of 2-(2′-Hydroxybenzoyl)pyrrole. A new synthesis of bioactive analogs of mono-deoxypyoluteorin. *J Heterocyclic Chem.* 1994;31(4):941–945. https://doi.org/10.1002/jhet.5570310442.
13. Schillaci D, Maggio B, Petruso S. In vitro activity of synthetic bromo analogs of pyrrolomycins against clinical staphylococcus aureus strains. *Pharmazie.* 1996;51(1):64.
14. Koyama M, Ezaki N, Tsuruoka T, Inouye S. Structural studies on pyrrolomycins C D and E. *J Antibiot.* 1983;36(11):1483–1489. https://doi.org/10.7164/antibiotics.36.1483.
15. Carter GT, Nietsche JA, Goodman JJ, et al. LL-F42248α, A novel chlorinated pyrrole antibiotic. *J Antibiot.* 1987;40(2):233–236. https://doi.org/10.7164/antibiotics.40.233.
16. Koyama M, Kodama Y, Tsuruoka T, Ezaki N, Niwa T, Inouye S. Structure and synthesis of pyrrolomycin A, a chlorinated nitro-pyrrole antibiotic. *J Antibiot.* 1981;34(12):1569–1576. https://doi.org/10.7164/antibiotics.34.1569.
17. Kaneda M, Nakamura S, Ezaki N, Iitaka Y. Structure of pyrrolomycin B, a chlorinated nitro-pyrrole antibiotic. *J Antibiot.* 1981;34(10):1366–1368. https://doi.org/10.7164/antibiotics.34.1366.
18. Ezaki N, Koyama M, Shomura T, Tsuruoka T, Inouye S. Pyrrolomycins C, D and E new members of pyrrolomycins. *J Antibiot.* 1983;36(10):1263–1267. https://doi.org/10.7164/antibiotics.36.1263.
19. Ezaki N, Koyama M, Kodama Y, et al. Pyrrolomycins F1, F2a, F2b and F3, new metabolites produced by the addition of bromide to the fermentation. *J Antibiot.* 1983;34(11):1431–1438. https://doi.org/10.7164/antibiotics.36.1431.
20. Charan RD, Schlingmann G, Bernan VS, Feng X, Carter GT. Dioxapyrrolomycin biosynthesis in streptomyces fumanus. *J Nat Prod.* 2006;69(1):29–33. https://doi.org/10.1021/np0503404.
21. Schillaci D, Petruso S, Sciortino V. 3,4,5,3',5'-Pentabromo-2-(2'-hydroxybenzoyl) pyrrole: a potential lead compound as anti-gram-positive and anti-biofilm agent. *Int J Antimicrob Agents.* 2005;25(4):338–340. https://doi.org/10.1016/j.ijantimicag.2004.11.014.
22. Raimondi MV, Cascioferro S, Schillaci D, Petruso S. Synthesis and antimicrobial activity of new bromine-rich pyrrole derivatives related to monodeoxypyoluteorin. *Eur J Med Chem.* 2006;41(12):1439–1445. https://doi.org/10.1016/j.ejmech.2006.07.009.
23. Raimondi MV, Schillaci D, Petruso S. Synthesis and anti-staphylococcal activity of new halogenated pyrroles related to pyrrolomycins F. *J Heterocyclic Chem.* 2007;44(6):1407–1411. https://doi.org/10.1002/jhet.5570440626.
24. Renneberg B, Kellner M, Laatsch H. Synthese halogenierter benzyl-und benzoylpyrrole. *Liebigs Ann Chem.* 1993:847–852. https://doi.org/10.1002/jlac.1993199301134.
25. Hodge P, Rickards RWJ. The halogenation of methyl pyrrole-2-carboxylate and of some related pyrroles. *Chem Soc.* 1965:459–470. https://doi.org/10.1039/JR9650000459 and references therein cited.
26. Schillaci D, Petruso S, Cascioferro S, Raimondi MV, Haagensen Ja.J, Molin S. In vitro anti-gram-positive and antistaphylococcal biofilm activity of newly halogenated pyrroles related to pyrrolomycins. *Int J Antimicrob Agents.* 2008;31(4):380–382. https://doi.org/10.1016/j.ijantimicag.2007.10.013.
27. Schillaci D, Petruso S, Raimondi MV, et al. Pyrrolomycins as potential anti-staphylococcal biofilms agents. *Biofouling.* 2010;26(4):433–438. https://doi.org/10.1080/08927011003718673.
28. Cascioferro S, Raimondi MV, Cusimano MG, et al. Pharmaceutical potential of synthetic and natural pyrrolomycins. *Molecules.* 2015;20(12):21658–21671. https://doi.org/10.3390/molecules201219797.
29. Rossino G, Raimondi MV, Rui M, et al. 400/cerium ammonium nitrate combined with microwave-assisted synthesis for rapid access to beta-amino ketones. an easy-to-use protocol for discovering new hit compounds. *Molecules.* 2018;23((4), 775):1–12. https://doi.org/10.3390/molecules23040775.
30. Zong Y, Bice TW, Ton-That H, Schneewind O, Narayana SV. Crystal structures of *Staphylococcus aureus* sortase A and its substrate complex. *J Biol Chem.* 2004;279:31383–31389. https://doi.org/10.1074/jbc.M401374200.
31. Cascioferro S, Totsika M, Schillaci D, Sortase A. An ideal target for antivirulence drug development. *Microb Pathog.* 2014;77C. https://doi.org/10.1016/j.micpath.2014.10.007 105e112.
32. Sahukhal GS, Batte JL, Elasri MO. msaABCR operon positively regulates biofilm development by repressing proteases and autolysis in *Staphylococcus aureus*. Nakane A, ed. *FEMS Microbiol Lett.* 2015;362(4):1–10.
33. Bose JL, Lehman MK, Fey PD, Bayles KW. Contribution of the *Staphylococcus aureus* Atl AM and GL murein hydrolase activities in cell division, autolysis, and biofilm formation. e42244 *PLoS ONE.* 2012;7(7) https://doi.org/10.1371/journal.pone.0042244.
34. Oshida T, Sugai M, Komatsuzawa H, Hong YM, Suginaka H, et al. A Staphylococcus aureus autolysin that has an N-acetylmuramoyl-L-alanine amidase domain and an endo-beta-N-acetylglucosaminidase domain: cloning, sequence analysis, and characterization. *Proc Natl Acad Sci USA.* 1995;92:285–289.
35. Hanwell MD, Curtis DE, Lonie DC, Vandermeersch T, Zurek E, Hutchison GR. Avogadro an advanced semantic chemical editor, visualization, and analysis platform. *J Cheminform.* 2012;4(1):1–17. https://doi.org/10.1186/1758-2946-4-17.
36. Maestro, Schrödinger, LLC, New York, NY, 2017, version 11.4.011.
37. Berman HM, Westbrook J, Feng Z, et al. The protein data bank. *Nucleic Acids Res.* 2000;28:235–242.
38. Pettersen EF, Goddard TD, Huang CC, et al. UCSF Chimera—A visualization system for exploratory research and analysis. *J Comput Chem.* 2004;25:1605–1612. https://doi.org/10.1002/jcc.20084.
39. Trott O, Olson AJ. *J Comput Chem.* 2010;31:455–461. https://doi.org/10.1002/jcc.21334.
40. Maggio B, Raffa D, Raimondi MV, et al. Discovery of a new class of sortase a transpeptidase inhibitors to tackle gram-positive pathogens: 2-(2-phenylhydrazinylidene)alkanoic acids and related derivatives. *Molecules.* 2016;21(2):241–256. https://doi.org/10.3390/molecules21020241.
41. Cascioferro S, Maggio B, Raffa D, Raimondi MV, Cusimano MG, Schillaci D, Manachini B, Leonchiks A, Daidone G. A new class of phenylhydrazinylidene derivatives as inhibitors of Staphylococcus aureus biofilm formation. *Med Chem Res.* 2016;255:870–878. https://doi.org/10.1007/s00044-016-1535-9.
42. Rueden CT, Schindelin J, Hiner MC. Image J2: imageJ for the next generation of scientific image data. *BMC Bioinf.* 2017;18:529https://doi:10.1186/s12859-017-1934-z.